Journal of ELECTRONIC MATERIALS, Vol. 38, No. 2, 2009
DOI: 10.1007/s11664-008-0580-7
© 2008 TMS
Regular Issue Paper

Interfacial Reaction Between Eutectic Sn-Pb Solder and Electroplated-Ni as well as Electroless-Ni Metallization During Reflow

HSIAO-YUN CHEN[1] and CHIH CHEN[1,2]

1.—Department of Materials Science and Engineering, National Chiao Tung University, Hsin-chu 30010, Taiwan, Republic of China. 2.—e-mail: chih@faculty.nctu.edu.tw

Electroplated-Ni (EP-Ni) has been adopted gradually as an underbump metallization layer due to its comparatively lower resistivity and higher deposition rate. In this study, the metallurgical reaction between eutectic Sn-Pb solder and EP-Ni as well as electroless-Ni (EL-Ni) was investigated at 200°C, 210°C, 220°C, and 240°C. It is found that the growth rate of Ni_3Sn_4 intermetallic compound (IMC) on EP-Ni was slower than that on EL-Ni. The consumption rate is measured to be 0.97×10^{-3} μm/s and 1.48×10^{-3} μm/s for EP-Ni and EL-Ni, respectively. The activation energy is determined to be 51 kJ/mol and 48 kJ/mol for EP-Ni and EL-Ni, respectively. The dense structure of EP-Ni may be responsible for the lower IMC formation rate.

Key words: Flip-chip solder joints, electronic packaging, electroplated Ni

INTRODUCTION

Solder bumps in flip-chip technology have been adopted in the microelectronic industry as interconnections due to their excellent electrical performance, thermal dissipation, and reliability.[1] A reliable solder joint can be formed by metallurgical reaction between molten solders and underbump metallization (UBM) on a chip or metallization on the substrate, which produces stable intermetallic compounds (IMCs) at joint interfaces.[2] During the soldering process, the formation of IMCs between solder alloys and the metallization layer is inevitable. The growth of these IMCs can strongly affect the mechanical reliability of solder joints.[3–5] As a result, selection of appropriate UBM plays an important role in developing a reliable flip-chip joint, especially so with the adoption of lead-free solders due to environmental concerns. A typical issue encountered in Pb-free adoption is that these Sn-based lead-free solders are found to be incompatible with traditional Cu-based metallization due to rapid reaction and spalling of Cu-Sn IMCs.[6,7] Instead, Ni-based UBM, such as electroless Ni-P alloy and pure Ni, have attracted much attention in recent years because of their good wettability,[8] good diffusion barrier ability, and slow reaction rate with solders.[5,9] Many studies have been published on the interaction between Ni-P and Sn-based solders,[10–21] examining the formation and growth of IMCs at the interface of molten solder and Ni-P UBM, solder reaction-assisted crystallization of Ni-P alloy, and the effect of IMCs on the mechanical properties of solder joints.

In recent years, electroplated-Ni (EP-Ni) thick film has been adopted as the UBM structure due to its comparatively lower resistivity and higher deposition rate. The resistivity of electroless-Ni(P) alloy may exceed 100 $\mu\Omega$ cm when the content of phosphorous reaches 12% or above, since Pb-free solders have a higher reaction during the reflow process, thus the thickness of the Ni(P) layer exceeds 10 μm in general, resulting in a much higher bump resistance. On the contrary, EP-Ni has a much lower resistivity of 6.8 $\mu\Omega$ cm. Therefore it has been adopted as a UBM material. The interfacial reactions between eutectic Sn-Pb solder and Ni foil have been studied.[9] A few studies on the interfacial reactions between Sn-Ag solder and

(Received January 17, 2008; accepted September 26, 2008; published online October 21, 2008)

electroplated-Ni have been conducted,[22,23] while the metallurgical reaction between eutectic Sn-Pb solders and EP-Ni has not been investigated in detail.[24,25] In particular, the consumption rate of the EP-Ni film and the activation energy of IMC formation merit further exploration.

In this study, interfacial reactions between eutectic Sn-Pb solders and EP-Ni have been investigated. The Ni consumption rate, IMC growth rate, and activation energy for the interfacial reaction have been determined. In addition, the interfacial reactions between the solders and electroless-Ni(P) (EL-Ni) were also studied at the same time. Thus, this paper provides direct comparisons of the soldering reaction between the two interfaces in samples of flip-chip scale.

EXPERIMENTAL

A schematic of the solder joint used in this study is shown in Fig. 1. On the chip side, 0.1-μm-thick titanium was sputtered onto the oxidized Si wafer to serve as a good adhesion layer. Copper of 0.5 μm thickness was then sputtered on the Ti layer and served as a seed layer for the subsequent electroplating process. After that, 5-μm Cu and 3-μm Ni layers were electroplated on the Ti/Cu layers as a UBM layer. Photolithography was employed to define the contact opening on the chip-side for solder electroplating of eutectic Sn-Pb solders. The Sn-Pb solder bumps were formed by reflowing in an infrared oven at 220°C for about 1 min. Then the bumped dies were mounted onto a FR5 substrate, in which the pad metallization on the substrate side was 5-μm electroless-Ni on the 30-μm-thick Cu lines. The solder bumps experienced another reflow during the mounting process.

For metallurgical reaction at the liquid state, the Sn-Pb packages were reflowed at different temperatures and for different durations. They were reflowed at 200°C, 210°C, 220°C, and 240°C on a hot plate for 5 min, 10 min, 1 h, 4 h, 6.25 h, and 9 h, respectively. The Si side was placed on the surface of the hot plate, so that the temperature in the solder was close to that of the hot-plate surface.

The microstructure of the interfacial regions between the solders and the Ni-based UBMs were examined by scanning electron microscope (SEM, JEOL 6500). A backscattered electron image (BEI) of SEM was employed to examine the morphology of the cross-sectional Sn-Pb samples. Moreover, the compositions of the solder joints and the IMCs were analyzed quantitatively by energy-dispersive spectroscopy and an electron probe microanalyzer

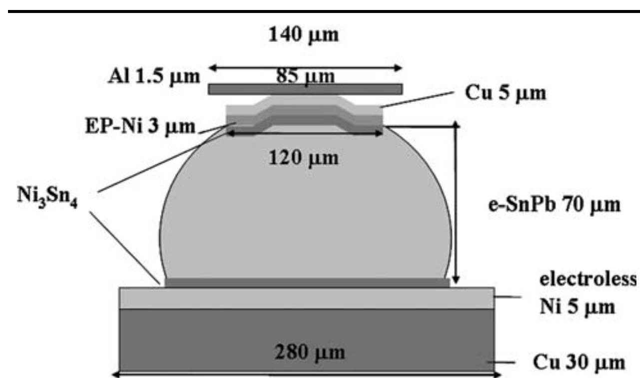

Fig. 1. Schematic structure for solder joints used in this study. EP-Ni was adopted on the chip side and EL-Ni was fabricated on the substrate side.

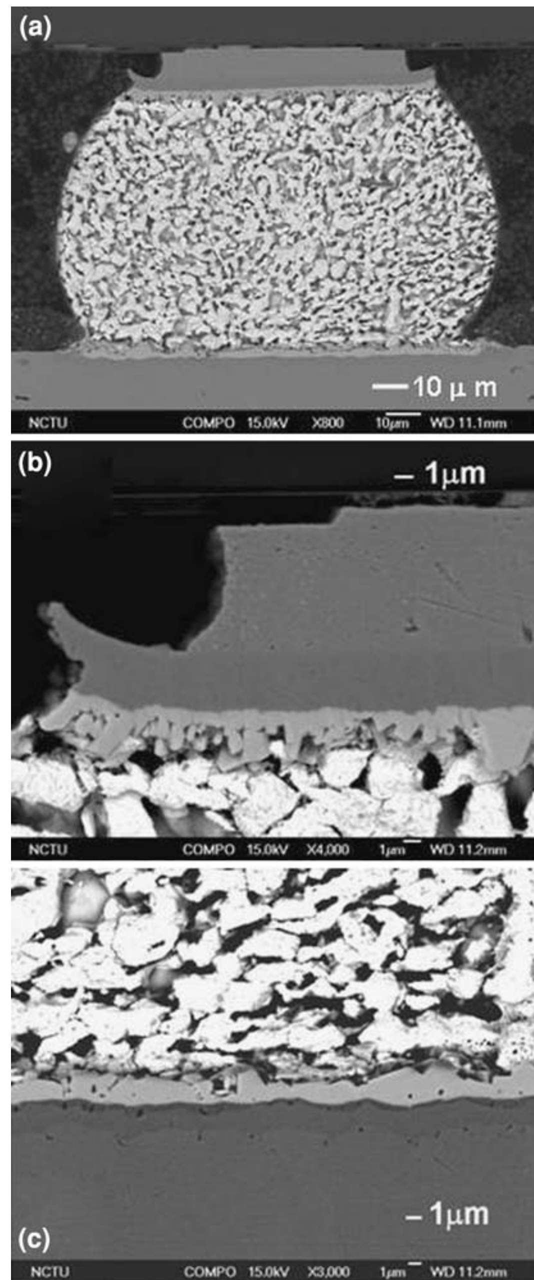

Fig. 2. Cross-sectional SEM images showing morphology of Ni_3Sn_4 IMCs in Sn-Pb solder with EP-Ni UBM and EL-Ni(P) metallization (a) for whole bump, (b) enlarged view of EP-Ni on the chip side, and (c) enlarged view of EL-Ni on the substrate side.

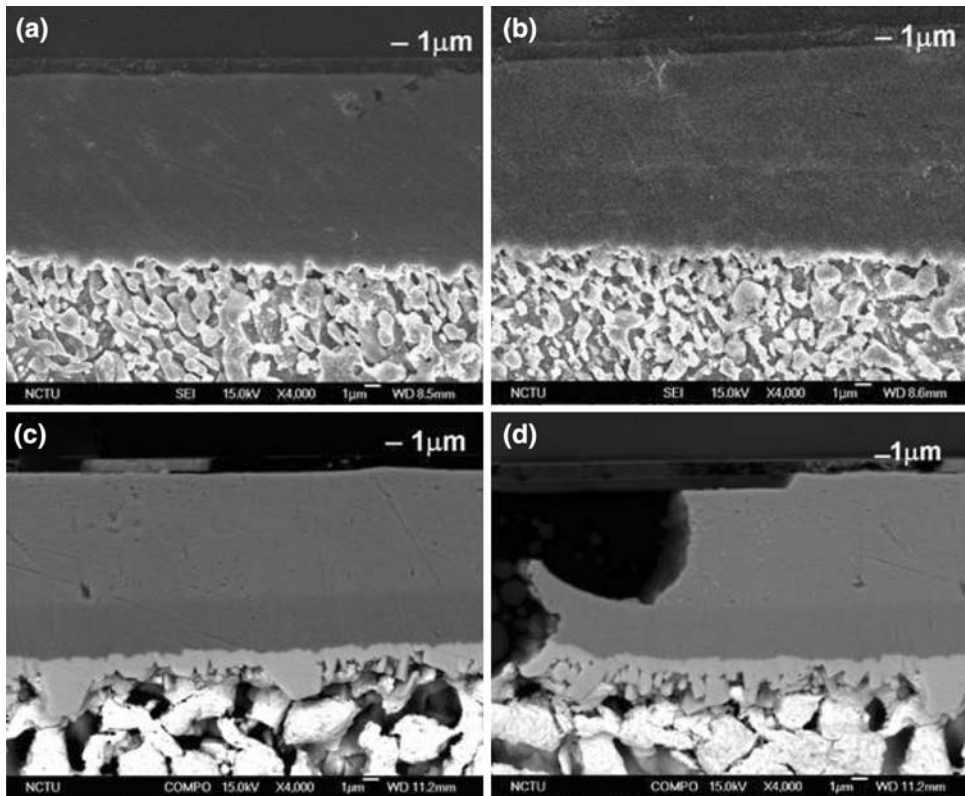

Fig. 3. Cross-sectional SEM images showing morphology of Ni_3Sn_4 IMCs at interface of Sn-Pb solder and EP-Ni UBM reflowed at 210°C for (a) 5 min, (b) 10 min, (c) 1 h, and (d) 9 h.

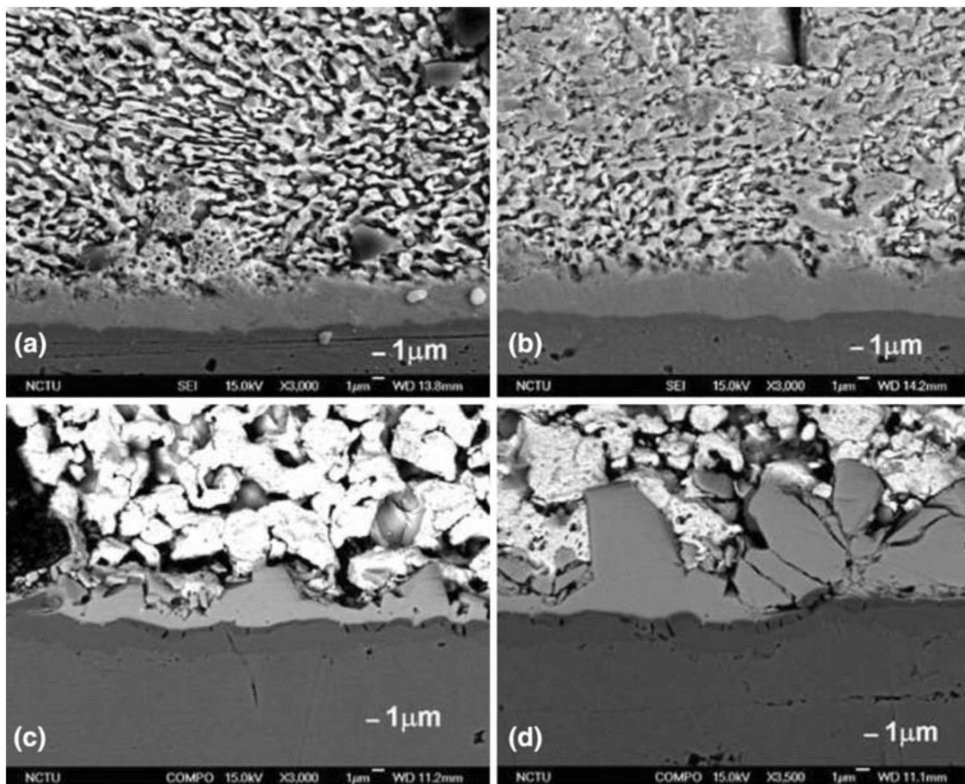

Fig. 4. Cross-sectional SEM images showing morphology of Ni_3Sn_4 IMCs at the interface of Sn-Pb solder and EL-Ni UBM reflowed at 210°C for (a) 5 min, (b) 10 min, (c) 1 h, and (d) 9 h.

(JXA-8800M, JEOL). A solution of nitride acid and acetone at a ratio of 49:1 was used for the selective etching of Sn to facilitate observation of the interface. The thickness of the IMC was calculated by commercial Matrox Inspector software. To obtain the average IMC thickness, six bumps were measured for each condition. The IMC thickness of each bump was measured 25 times by the software in order to minimize artificial errors.

RESULTS AND DISCUSSION

EP-Ni was found to possess a lower reaction rate with the Sn-Pb solder. Figure 2a shows a cross-sectional BEI SEM image for the as-fabricated sample. Even though the interface of the EP-Ni and solder on the chip side experienced about 1 min longer than the EL-Ni(P)/solder interface on the substrate side, the Ni_3Sn_4 IMC layer at the EP-Ni/solder was thinner. It was 0.90 μm at the EP-Ni/solder interface, but it was 1.20 μm at the EL-Ni/solder interface. IMC morphology reveals that it is rougher at the EP-Ni/solder interface, as shown in Fig. 2b and c. The reason for this difference remains unclear. As the reflow time increased, the thickness of the IMC also increased. Figure 3a–d displays SEM images at the EP-Ni side for Sn-Pb joints reflowed at 210°C for 5 min, 10 min, 1 h, and 9 h, respectively. The thickness of the IMC increased to 0.93 μm, 0.93 μm, 1.80 μm, and 2.86 μm under the four conditions, respectively. These results indicate that the reaction rate is very low between EP-Ni and the eutectic Sn-Pb solder. On the other hand, the interfacial structures at the EL-Ni end for the above four reflow conditions are shown in Fig. 4a–d. The thickness of the IMC increased to 1.32 μm, 1.39 μm, 3.27 μm, and 4.38 μm for the sample reflowed for 5 min, 10 min, 1 h, and 9 h, respectively. Again, the IMC layer was thinner on the EP-Ni side for all the four conditions.

A NiSnP layer was detected between the Ni_3Sn_4 IMC and the Ni_3P layer, as shown in Fig. 5a. Voids were frequently observed in the Ni_3P layer, as indicated by the arrows in Fig. 5b. These Kirkendall voids have been reported in previous studies.[9,26,27] The presence of Kirkendall voids indicates that an unbalanced flux had occurred in the system, with Ni atoms diffusing into the solder to form Ni_3Sn_4 IMCs. Furthermore, we found that the amount of voids increased with an increase in reflow time and temperature. On the other hand, no voids were found at the Ni_3Sn_4/EP-Ni interface, and the interface remained almost the same regardless of the reflow temperature and duration, except that the IMC layer grew thicker. The IMC layer on the EP-Ni side did not spall into the solder for all the reflow conditions. On the contrary, some Ni_3Sn_4 IMCs were observed inside the solder of the remaining Ni(P) layer. He et al.[27] reported that the stress, generated during the formation of IMCs through the liquid–solid reaction, caused the IMCs to spall from the Ni(P) UBM.

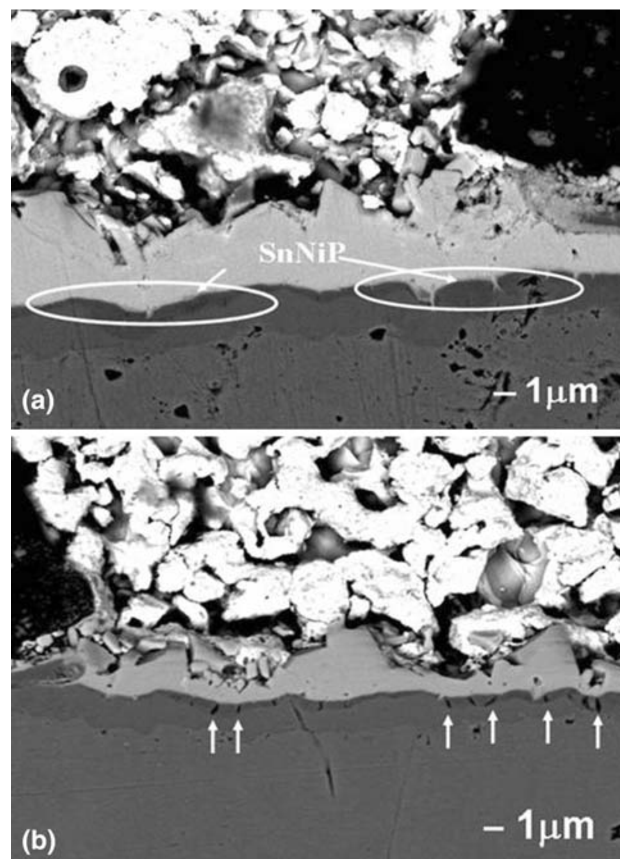

Fig. 5. (a) Enlarged BEI SEM image on the substrate side showing the IMCs, NiSnP, Ni_3P, and the remaining Ni(P) layer after being reflowed at 210°C for 1 h, and (b) numerous voids were observed in the Ni_3P layer, indicated by arrows.

The average thickness of the IMC measured for all the reflow conditions are listed in Table I for all the reflowing conditions. The growth kinetics of the continuous intermetallic layer (Ni_3Sn_4) can be expressed by an empirical power law, which describes the average intermetallic thickness (h) as a function of time (t) and temperature (T):

$$h(t,T) = h_0 + k_h \exp\left(-\frac{Q_h}{RT}\right) t^{1/n}, \quad (1)$$

where h_0 is the initial intermetallic thickness, k_h and n are constants, Q_h is the apparent activation energy for the thickening process, and R is the universal gas constant. The fitting of the experimental data is shown in Fig. 6, which yields an n value of 4.07 and 3.66 for the EP-Ni and EL-Ni system, respectively. The values appear slightly bigger than that of 3.14 reported by Ghosh[24] for Ni_3Sn_4 scallops formed in Sn-38Pb/Ni samples at 200°C to 250°C for 5 min. The measured n value is greater than 3.0 for the thickening kinetics of Ni_3Sn_4 IMCs formed in both systems. The thickening process of Ni_3Sn_4 for both EP-Ni and EL-Ni

Table I. Average Thickness of Ni_3Sn_4 for Various Reflow Conditions

	5 min (μm)	10 min (μm)	1 h (μm)	4 h (μm)	6.25 h (μm)	9 h (μm)
200°C EP-Ni	0.94	0.93	1.60			
200°C EL-Ni	1.26	1.3	2.80			
210°C EP-Ni	0.93	0.93	1.80	2.14	2.47	2.86
210°C EL-Ni	1.32	1.39	3.27	3.88	4.12	4.38
220°C EP-Ni	0.98	0.94	2.09			
220°C EL-Ni	1.39	1.43	3.56			

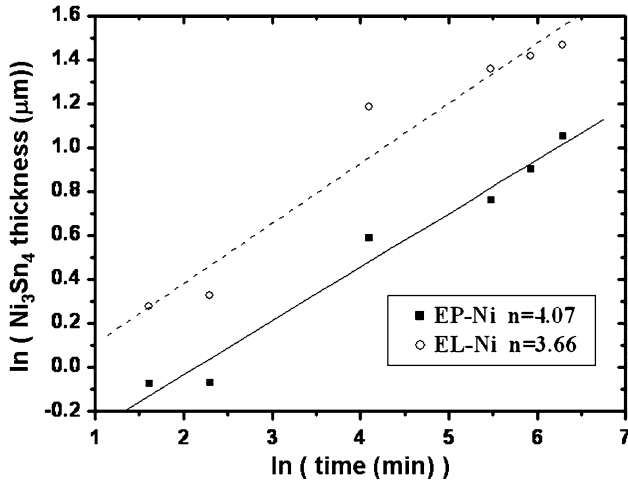

Fig. 6. The fitting curve of the time exponent for parameter n value of the IMC thickening process.

systems in this study differs from diffusion-controlled growth, which predicts $t^{1/2}$ growth kinetics,[24,28,29] and from scallop coarsening by a ripening process with thickness proportional to $t^{1/3}$.[30] According to Ghosh, the thickening kinetics of Ni_3Sn_4 scallops is related to the radial growth kinetics, and grain boundary diffusion may play an important role in the thickening kinetics. Thus, the kinetics in this study may be governed by grain boundary diffusion.

To calculate the activation energy for the Ni_3Sn_4 IMC formation on EP-Ni and EL-Ni(P) UBMs, one can use the Arrhenius plot shown in Fig. 7a using the thickness data at 1 h of reflow time. The activation energy for EP-Ni UBM is measured to be 51 kJ/mol, whereas it is 48 kJ/mol for EL-Ni UBM. Compared with the results for the eutectic Sn-Pb solder on Ni foil reported by Kim et al.,[9] as shown in Fig. 7b, the activation energy they obtained using the data for 5 min and 10 min of reflow time ranges from 47 kJ/mol to 32 kJ/mol using the data for 5 min and 10 min of reflow time. The values we obtained are slightly higher. In addition, these values are much higher than those reported by Kang and Ramachandran[2] for Ni reacting with liquid Sn at 300°C to 520°C. The values they obtained lie between 13 kJ/mol and 17 kJ/mol. In addition, Gun and Bamberger also reported that activation energy for diffusion of Ni in liquid Sn is 27.6 ± 1.7 kJ/mol

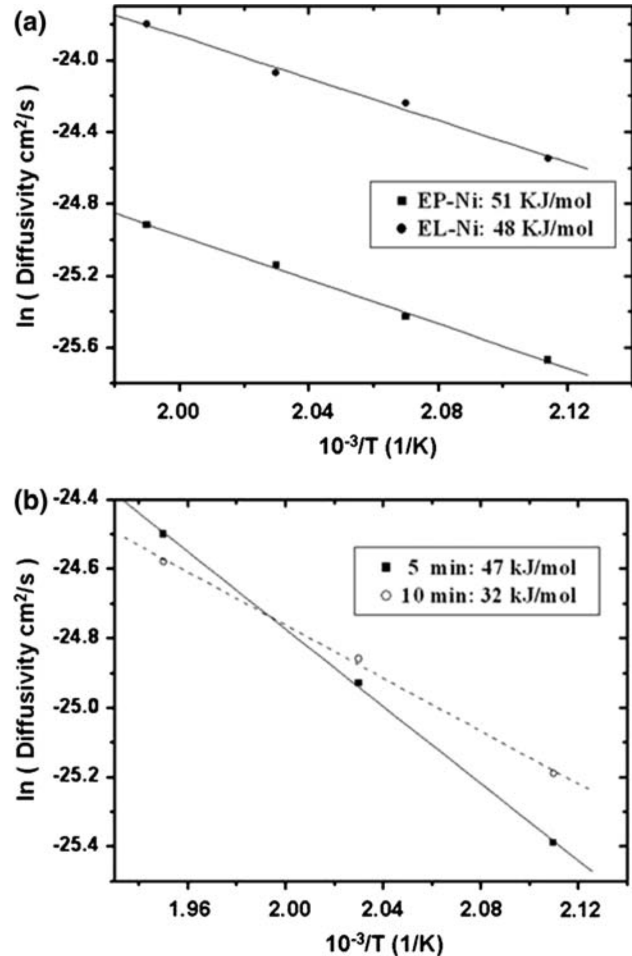

Fig. 7. (a) Arrhenius plot for metallization of both EP-Ni and EL-Ni using the data at 1 h of reflow duration. The activation energies were determined to be 51 kJ/mol and 48 kJ/mol for the IMC growth on EP-Ni and EL-Ni, respectively. (b) Arrhenius plot for the results published by Kim et al.,[9] which is for eutectic Sn-Pb solder on bulk Ni. Data from reflow durations of both 5 min and 10 min were used.

in the temperature range of 235°C to 600°C.[31] Thus the activation for eutectic Sn-Pb on Ni is much higher than that for pure Sn on Ni.

In order to determine the different consumption rates of EP-Ni and EL-Ni, we assume that the total loss of Ni was equal to the summation of Ni in Ni_3Sn_4 and in the liquid solder. From the mass balance of Ni, the consumed thickness of Ni is:

$$\Delta h = \frac{1}{\rho_{\mathrm{Ni}} A}\left(\frac{nV}{100}\rho_{\mathrm{L}} + f_{\mathrm{Ni}}\rho_{\mathrm{C}} V_{\mathrm{C}}\right), \quad (2)$$

where A is the total interfacial area between solder and Ni, n is the wt.% of Ni in liquid solder, V is the total volume of liquid solder, f_{Ni} is the weight fraction of Ni in the Ni_3Sn_4 compound, t_{C} is the thickness of Ni_3Sn_4, and ρ_{Ni}, ρ_{L}, and ρ_{C}, are the density of the Ni, liquid solder, and Ni_3Sn_4 compound, respectively. After the saturation of Ni in the molten solder, the consumption rate of Ni varies with the change in volume of Ni_3Sn_4 compounds, and the rate equation is then given by:

$$\frac{\mathrm{d}h}{\mathrm{d}t} = f_{\mathrm{Ni}} \frac{\rho_{\mathrm{C}}}{\rho_{\mathrm{Ni}}} \frac{\mathrm{d}t_{\mathrm{C}}}{\mathrm{d}t}. \quad (3)$$

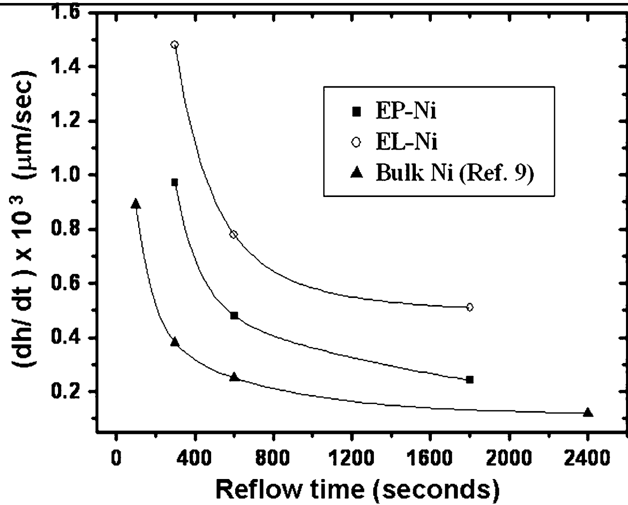

Fig. 8. Consumption rates of Ni layers as a function of reflow time at 240°C for eutectic Sn-Pb on EP-Ni, EL-Ni, and Ni foil.

Since the solubility of Ni in eutectic Sn-Pb solder between 200°C and 240°C is very small, the value of n in Eq. 2 is very small. The consumption rates of Ni at 240°C are shown in Fig. 8, which are 0.97×10^{-3} μm/s for EP-Ni and 1.48×10^{-3} μm/s for EL-Ni for 5 min of reflow time when the rates are assumed to be linear within 5 min. In general, EP-Ni has a more dense structure than EL-Ni, which may be responsible for the slower Ni consumption rate for EP-Ni. Furthermore, compared with that reported by Kim et al., the consumption rate for Sn-Pb solder reacting with Ni foil at 240°C within 10 min is 0.38×10^{-3} μm/s.[9] The consumption rate for the bulk Ni is also shown in the figure. The lower consumption rate for the Ni foil may be attributed to its dense structure. Thus EP-Ni and EL-Ni have higher reaction rates than the Ni foil with molten Sn-Pb solder. It is not clear at this moment why the measured activation energies for Ni_3Sn_4 IMCs on EP-Ni and EL-Ni UBMs were almost the same, but the growth rates of IMCs exhibit significant variation. According to Eq. 1, the difference in growth rate may

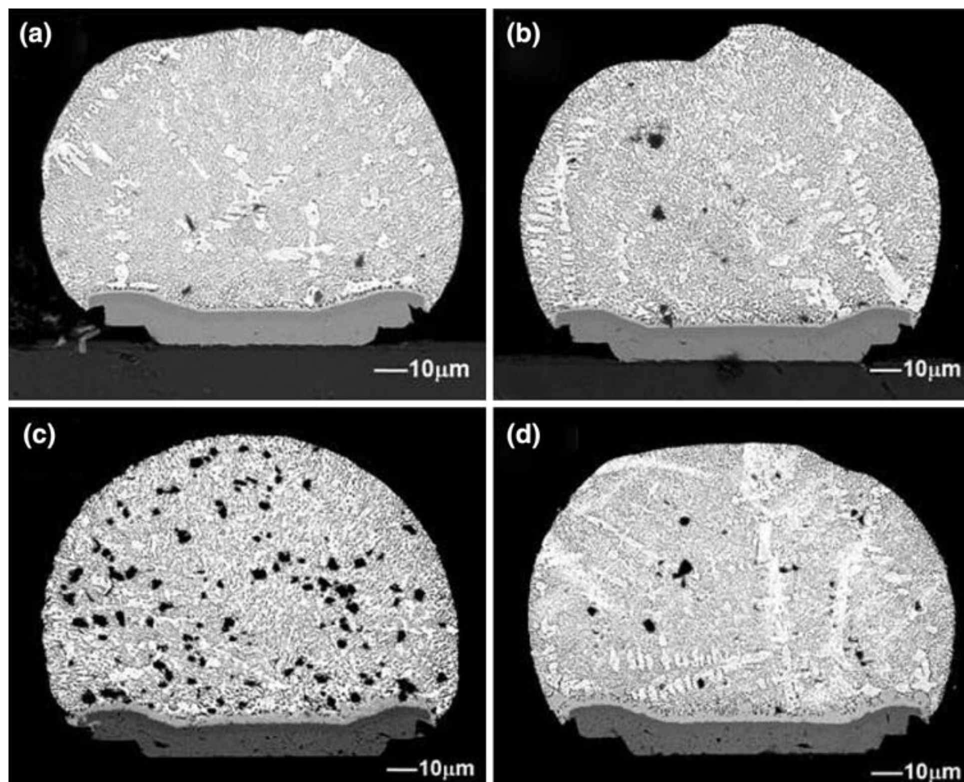

Fig. 9. Cross-sectional SEM images showing morphology of Ni_3Sn_4 IMCs at the interface of the Sn-Pb solder and the EP-Ni UBM reflowed at 210°C for (a) 5 min, (b) 10 min, (c) 1 h, and (d) 9 h.

Table II. Average Thickness of Ni_3Sn_4 for Bumped-die Samples Reflowed at 210°C for Various Durations

	5 min (μm)	10 min (μm)	1 h (μm)	9 h (μm)
IMC thickness on EP-Ni (μm)	0.88	1.02	2.27	3.01
Calculated EP-Ni consumed thickness	0.26	0.31	0.68	0.90
Direct measured EP-Ni consumed thickness	0.30	0.37	0.73	1.02
Calculated EP-Ni consumed thickness for flip-chip samples	0.27	0.29	0.54	0.89

result from the constant K_h. The kinetics in liquid-state reactions may be very complicated. It is speculated that EP-Ni has a more dense structure than EL-Ni, resulting in different values of the constant K_h.

To investigate whether the presence of EL-Ni on the substrate affects the formation of Ni_3Sn_4 IMCs on the chip end, the metallurgical reaction in bump-die samples was also studied as shown in Fig. 9a through d. Table II shows the IMC thickness of both the IMC layer and the consumed EP-Ni. The thickness of the consumed EP-Ni is 0.30 μm, 0.37 μm, 0.73 μm, and 1.02 μm after reflow at 210°C for 5 min, 10 min, 1 h, and 9 h, respectively. The rate of consumption of EP-Ni in bumped-die samples at 210°C is 1.0×10^{-3} μm/s after reflow at 210°C for 5 min. The EP-Ni consumption rates of bumped-die samples are very close to those of flip-chip samples. These results imply that the presence of EL-Ni on the substrate end has little effect on the IMC formation on the chip end, which may be attributed to the very small Ni solubility in the eutectic Sn-Pb solder. Therefore, the measured Ni consumption rate in flip-chip samples is quite close to that in bumped-die samples.

CONCLUSION

The liquid-state reaction between Sn-Pb and EP-Ni as well as EL-Ni has been studied under various reflow conditions. By fabricating EP-Ni on the substrate side and EL-Ni on the chip side, direct comparison on the growth of Ni_3Sn_4 can be made. The growth rate of IMCs on EL-Ni was faster for all the reflow conditions. The consumption rate has been measured to be 0.97×10^{-3} μm/s and 1.48×10^{-3} μm/s for EP-Ni and EL-Ni, respectively. The activation energy has been determined to be 51 kJ/mol and 48 kJ/mol for EP-Ni and EL-Ni within 10 min of reflow time, respectively.

ACKNOWLEDGEMENT

The authors would like to thank the National Science Council of R.O·C. for the financial support under Grant No. 95-2221-E-009-088MY3.

REFERENCES

1. R.R. Tummala, E.J. Rymaszewski, and A.G. Klopfenstein, *Microelectronics Packaging Handbook*, 2nd ed., Part 2, Ch 8. (New York: Chapman & Hall, 1997).
2. S.K. Kang and V. Ramachandran, *Scr. Mater.* 14, 421 (1980).
3. M.O. Alam, Y.C. Chan, and K.C. Hung, *J. Electron. Mater.* 31, 1117 (2002). doi:10.1007/s11664-002-0051-5.
4. K.H. Prakash and T. Sritharan, *J. Electron. Mater.* 32, 939 (2003). doi:10.1007/s11664-003-0227-7.
5. K.N. Tu and K. Zeng, *Mater. Sci. Eng. R* 34, 1 (2001).
6. H.K. Kim, K.N. Tu, and P.A. Totta, *Appl. Phys. Lett.* 68, 2204 (1996). doi:10.1063/1.116013.
7. K. Zeng and K.N. Tu, *Mater. Sci. Eng. R* 38, 55 (2002).
8. R.J.K. Wassink, *Soldering in Electronics* (IOM: Electrochemical Publications, 1984).
9. P.G. Kim, J.W. Jang, T.Y. Lee, and K.N. Tu, *J. Appl. Phys.* 86, 6746 (1999). doi:10.1063/1.371751.
10. K.L. Lin and Y.C. Liu, *IEEE Trans. Adv. Packag.* 22(4), 568 (1999). doi:10.1109/6040.803447.
11. Z. Mei and R.H. Dauskardt, *1999 MRS Spring Meeting Symposium M, Materails Reliability in Mocroelectronics IX*, pp. 1.
12. C.Y. Lee and K.L. Lin, *Thin solid films* 249, 201 (1994). doi:10.1016/0040-6090(94)90761-7.
13. J.W. Jang, P.G. Kim, and K.N. Tu, *J. Appl. Phys.* 85, 12–8456 (1999). doi:10.1063/1.370627.
14. K.C. Hung, Y.C. Chen, C.W. Tang, and H.C. Ong, *J. Mater. Res.* 15, 11–2534 (2000). doi:10.1557/JMR.2000.0363.
15. K.C. Hung and Y.C. Chen, *J. Mater. Sci. Lett.* 19, 1755 (2000). doi:10.1023/A:1006735103744.
16. J.W. Jang, D.R. Peter, T.Y. Lee, and K.N. Tu, *J. Appl. Phys.* 88, 6359 (2000). doi:10.1063/1.1321787.
17. Y.D. Jeon, K.W. Paik, K.S. Bok, W.S. Choi, and C.L. Cho, *IEEE 2001 Electronic Components and Technology Confernce*.
18. M. He, A. Kumar, P.T. Yeo, G.J. Qi, and Z. Chen, *Thin Solid Films* 462–463, 387 (2004). doi:10.1016/j.tsf.2004.05.062.
19. S.J. Wang, H.J. Kao, and C.Y. Liu, *J. Electron. Mater.* 30, 130 (2004).
20. S.J. Wang and C.Y. Liu, *Scr. Mater.* 49, 813 (2003). doi:10.1016/S1359-6462(03)00486-X.
21. M. He, W.H. Lau, G. Qi, and Z. Chen, *Thin Solid Films* 462–463, 376 (2004). doi:10.1016/j.tsf.2004.05.058.
22. C.P. Huang and C. Chen, *J. Mater. Res.* 20, 2772 (2005). doi:10.1557/JMR.2005.0334.
23. C.S. Huang, J.G. Duh, and Y.M. Chen, *J. Electron. Mater.* 32, 1509 (2003). doi:10.1007/s11664-003-0122-2.
24. G. Ghosh, *J. Appl. Phys.* 88, 6887 (2000). doi:10.1063/1.1321791.
25. G. Ghosh, *Acta Mater.* 48, 3719 (2000). doi:10.1016/S1359-6454(00)00165-8.
26. Y.D. Jeon, K.W. Paik, K.S. Bok, W.S. Choi, and C.L. Cho, *Electronic Components and Technology Conference* (San Diego, USA: IEEE, 2001), pp. 1326–1332.
27. M. He, Z. Chen, and G. Qi, *Acta Mater.* 52, 2047 (2004). doi:10.1016/j.actamat.2003.12.042.
28. Y. Takaku, X.J. Liu, I. Ohnuma, R. Kainuma, and K. Ishida, *Mater. Trans.* 45, 646 (2004). doi:10.2320/matertrans.45.646.
29. R.H. Dauskardt, F. Haubensak, and R.O. Ritchie, *Acta Metall. Mater.* 38, 143 (1990). doi:10.1016/0956-7151(90)90043-G.
30. H.K. Kim and K.N. Tu, *Phys. Rev. B.* 53, 16027 (1996). doi:10.1103/PhysRevB.53.16027.
31. D. Gur and M. Bamberger, *Acta Mater.* 46, 4917 (1998). doi:10.1016/S1359-6454(98)00192-X.